Available online at www.sciencedirect.com
SCIENCE DIRECT®
ELSEVIER
Powder Technology 163 (2006) 196 – 201
POWDER TECHNOLOGY
www.elsevier.com/locate/powtec

Granular components of cement: Influence of mixture composition

A.M. Vidales [a,*], I. Ippolito [b], O.A. Benegas [c], F. Aguirre [c], O.C. Nocera [c], M.R. Baudino [c]

[a] Departamento de Física y CONICET, Universidad Nacional de San Luis, Chacabuco 917, 5700 San Luis, Argentina
[b] Grupo de Medios Porosos y CONICET, Facultad de Ingeniería, Universidad de Buenos Aires, Paseo Colón 850, 1063 Buenos Aires, Argentina
[c] Departamento de Minería, Universidad Nacional de San Luis, Chacabuco 917, 5700 San Luis, Argentina

Received 18 October 2005; received in revised form 6 February 2006; accepted 17 February 2006
Available online 2 March 2006

Abstract

Raw granular materials used in cement manufacturing are limestone grains displaying a broad size distribution, ranging from microns to a couple of inches. They are stored as pyramidal heaps and, although empirical homogenization techniques are used with good results, there are important factors like segregation and grinding conditions that produce mixtures with different poorly controlled size. For this reason, the stability of the heaps strongly depends on these factors and it is important to study the influence of the respective amounts of particles of different sizes on the properties of the mixture. In this work, we report experiments analyzing the relationship between the characteristic angles of equilibrium of the heaps and the geometry, size and chemical composition of the grains. We also look for correlations between the values of the characteristic angles and the relative amounts of grains of different sizes that make up the materials.

We demonstrate that the chemical composition is correlated with the geometry of the grains and that their aspect ratio does not influence the critical angles. We also show that the critical angles mostly depend on the relative amount of fine grains in the granular mixture and on the dispersion of the sizes. The results obtained allow one to draw conclusions that may be relevant to the treatment and storage of raw materials in the cement industry.

Keywords: Granular piles; Angle of repose; Stability angles

1. Introduction

Dry granular materials have drawn a large amount of attention over the last fifteen years [1,2]. Their key part in many natural and industrial scenarios motivates the study of the Physics underlying them interesting, although apparently simple, complex problems have appeared.

Experiments shedding light on the basic behavior of these systems are the most important tools for characterizing and explaining the behavior of these multi-particle systems (in view of the extreme complexity of the physical parameters governing their dynamics). Furthermore, the increasing capabilities of numerical experiments have greatly helped to understand many of these phenomena.

The present work focuses on real industrial systems, namely heaps of limestone grains that represent the basic raw material for cement production. This raw material is stored as pyramidal heaps and, although empirical homogenization techniques are used with good results, segregation is observed due to the great difference between the grain sizes. In fact, segregation takes place every time this dry material is handled. On the other hand, there are another problems related to the fact that the range of sizes of the grains in these heaps is very broad (open particle size distribution). The relative amount of particles of a given size in the mixture is strongly related to the grinding process, and, particularly, to the degree of wear of the hammers used in the mills.

Although the treatment, handling and mixing of grains follows strictly standard industrial protocols (depending on the needs of the company), more basic studies are needed to characterize better the properties of the materials and improve the prediction of the behavior of the heaps as a function of their composition and stability.

In previous studies [3–5], the critical angles have extensively been studied in order to characterize the stability of the heaps and most of the works were related to the characteristics and dynamics

* Corresponding author. Tel.: +542652436151.
E-mail address: avidales@unsl.edu.ar (A.M. Vidales).

0032-5910/$ - see front matter © 2006 Elsevier B.V. All rights reserved.
doi:10.1016/j.powtec.2006.02.005

of the avalanches [5–9]. The stability of a packing of grains can be characterized by the *maximum angle of stability* θ_M (i.e. the angle at which the grains start to flow) and the *angle of repose* θ_R (i.e. the angle of the surface right after an avalanche). The stability of the packing is influenced by the number of layers, the packing length and the surrounding humidity.

Aguirre et al. [11] have shown that the *maximum angle of stability* θ_M depends on the initial packing fraction with higher θ_M values for denser packings. Once the avalanche starts, the process evolves displacing out a well defined quantity of mass and the final free surface always reaches the same angle θ_R. The angle θ_R is independent of θ_M and of the amount of mass displaced out: this indicates that θ_R is an intrinsic parameter of the granular medium as generally expected in the literature [10].

The objective of the present study is to characterize the stability of packings of limestone grains through experiments at the laboratory scale, using the same raw material as for manufacturing cement. The influence of the chemical composition is particularly studied. The stability of the heaps is analyzed by measuring the critical angles for packings corresponding to different distributions of grain sizes.

2. Experimental procedure and results

2.1. The grains

As is well known, similar rocks out of different quarries may have very different chemical compositions, size distributions and geometrical parameters. For this reason, we used four chemically different samples. These samples are made of raw material extracted out of four different mines belonging to a cement manufacturer. They will be labeled S1, S2, S3 and S4, respectively. Each sample Si associates grains from four subsets F_i, each of them corresponding to a given range of sizes ϕ: these ranges are defined as follows: $\phi>5$ cm (F1); 1.2 cm$<\phi<$5 cm (F2); 0.08 cm$<\phi<$1.2 cm (F3) and $\phi<$0.08 cm (F4). This provided a total of sixteen sub-samples. As is shown in the following, family F4 (powder) has an important influence on the critical angles.

The experimental procedure is the following: first, a chemical analysis of each sample is performed using standard fluorescence spectroscopy. Second, the flatness and elongation ratios are measured as a function of composition and size. These ratios are respectively defined as:

$$\alpha = \frac{T}{W}\ ;\ \beta = \frac{W}{L} \tag{1}$$

where T = characteristic thickness; W = characteristic width; and L = characteristic length of the grains. With this definition $\alpha=\beta=1$ corresponds to cubic grains.

Third, in order to compare the stability characteristics of different samples, two samples were selected and the critical angles (repose and maximum stability) for heaps with different distributions of grain sizes (different subsets) were measured. Finally, the influence of the relative amount of dust and large grains on the stability of the heaps has been investigated.

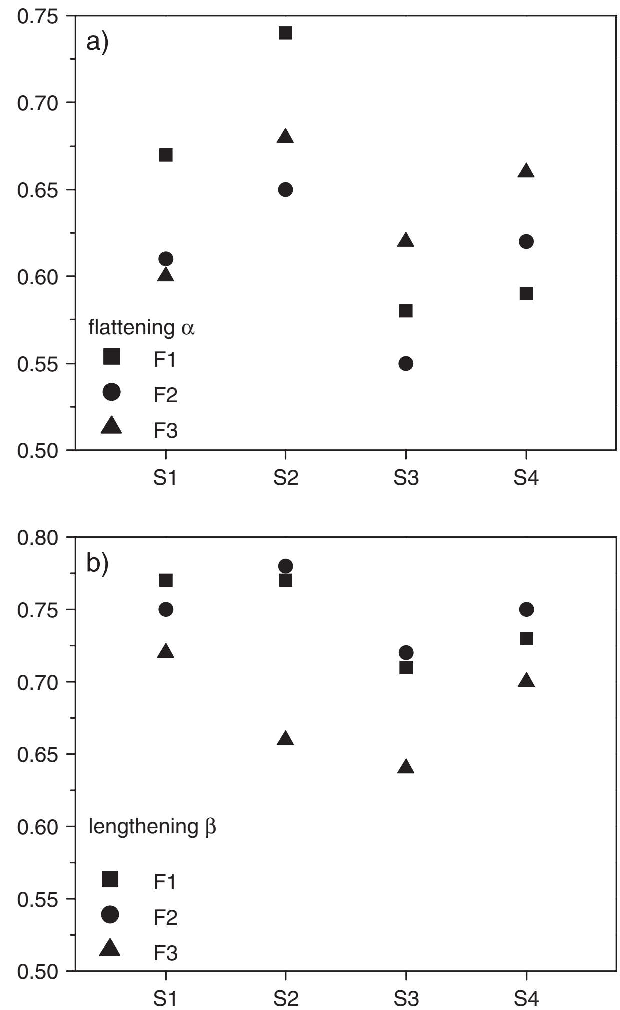

Fig. 1. Flatness and elongation ratios for all samples and subsets F1, F2 and F3 used in the experiments.

2.2. Chemical and shape characterization

For each sample Si and for all subsets F_i but for F4, we measure α and β, as defined above. L, T and W were measured directly with a caliper. For each subset F_i of a given sample, 30 different grains were selected at random after passing the sample a sieve. The length of a grain is taken equal to the largest dimension, the thickness to the smallest and the width to the intermediate one. After performing all measurements, the average values of the characteristic dimensions were computed for each subset with an error of the order of 5%.

The values of α and β obtained from these results are displayed in Fig. 1a and b. The geometry of the grains from sample S3 is the farthest from the cubic geometry (with characteristic ratios which differ most from 1). The grains from sample 2 are closest to a cubic geometry. In all samples, the elongation tends to increase for smaller grains while no such correlation is apparent for the flatness ratio.

An X-ray fluorescence technique has been used to determine the chemical composition of all samples and subsets. The most widespread components in each rock source are: SiO_2, CO_3,

Table 1
Percentage in weight of SiO_2

Size range	S1	S2	S3	S4
F4	11.54	7.20	16.35	23.11
F3	3.81	6.56	11.06	20.81
F2	4.54	2.96	10.98	18.67
F1	4.09	3.79	10.15	17.37
Mean [a]	6.00	5.13	12.14	19.99

[a] Over all families F_i.

Al_2O_3, Fe_2O_3, CaO and MgO. In all samples, the percentages of different minerals are strongly correlated to the grain sizes. Table 1 lists the percentage of SiO_2 measured in grains from each subset. This content increases as a function of the degree of grinding. The finest grains (F4) have the highest amount of silica: this result will depend on the procedure used to prepare and handle the powder. In order to estimate the impact of this result, one has to take into account the relative weight corresponding to subset F4: grains from this subset represent 20% of the total weight of each sample, which is a rather significant amount. As a result, any handling procedure that maintains a high volume of dust in the raw material contributes to improve the granular material sent to the manufacturing facility because a higher amount of silica will be present in it.

In order to further investigate the relation between the chemical composition and the ratios α and β, the amount of $CO_3^=$ in the samples is also included in Table 2 (note that a larger percentage of $CO_3^=$ indicates a higher fraction of limestone in a rock). On the other hand, a higher percentage of SiO_2 reflects an important influence of schists on the formation of the rocks. After crushing the rock, schists (which are mechanically less resistant) generate a larger percentage of finer grains (dust) than limestone and of flatter grains, especially in the F1 and F2 subsets. For low values of α and β, the grains present a flat shape which indicates that they were produced by the degradation of schists. This description is in good agreement with the values obtained for sample S2. Grains from this sample have both the most cubic-like geometry and, in most cases, the lowest content of SiO_2 (Table 1). Its $CO_3^=$ content is the highest among all samples.

On the contrary, sample S3 (low cubic index) includes a larger fraction of SiO_2 lower content of limestone than samples S1 and S2. Although, overall, the grains from sample S4 are closer to a cubic shape, those belonging to subsets F1 and F2 have a lower flatness index, indicating a similar chemical composition.

2.3. Critical angles

The experimental set-up includes a parallelepiped glass box (25×45×30 cm). One of the vertical walls can be removed and serves as a sliding gate (Fig. 2). The height of the packing was chosen large enough so that the bottom wall has no significant influence on the stability of the pile [6]. The box is fitted to a rotation axis and a goniometer allows measuring the angles with a precision of 0.5°. In order to determine the angles of stability and relate them to results presented above, we selected the two samples S1 and S3 (with all their subsets). These samples were chosen because they represent extreme cases for the values of the ratios α and β.

The granular packings are realized by pouring the grains and filling the box up to the level of the lateral wall.

Two angles are measured in these experiments: the angle of repose (θ_R) and the maximum angle of stability (θ_M).

The first one is determined in two ways (see Fig. 2 for a schematic representation).

1) First, the sample is placed inside a glass box (Fig. 2a). The container is carefully set horizontal. The sliding gate is then quickly moved upwards so that a certain amount of grains flows out of the system (Fig. 2b). A line following the slope of the surface is then plotted on the glass wall (Fig. 2c). The box is then tilted until this line becomes horizontal which allows reading directly the value of the angle of repose θ_{RT} on the goniometer.
2) The granular packing is prepared by filling up the box with grains right up to the level of the rim of the lateral wall (Fig. 2d) so that the height of the packing is well determined and grains are at the limit of flowing out. The box is initially horizontal and then carefully tilted at a constant rotation rate until an avalanche occurs (Fig. 2e). We mean by "avalanche" the first sudden simultaneous motion of several grain layers. The experiment is then stopped and the tilt angle of the container with respect to the horizontal is recorded. We also measure the slope of the surface after a new equilibrium has been reached (Fig. 2e). When the avalanche is triggered, the displaced material is always free to leave the container. In this way, the slope of the surface after the avalanche represents the angle of repose θ_R, and the tilt angle of the container provides the corresponding value of the maximum angle of stability θ_M. Experiments were performed at a low relative humidity, so that capillary and electrostatic effects are negligible.

It is worthy to mention here that, although each sample was carefully prepared in a similar way, repeating all the manipulations details, segregation by flux is always a likelihood process present both in the initial filling up of the glass box and during the discharge due to avalanches [12]. Nevertheless, it becomes very difficult to measure and characterize them in the present system [12,13]. Even more, segregation is always present in all manipulation stages of the cement industry and, in fact, it deserves a particular detailed study that is in progress at present. We will report on this issue elsewhere in the future.

Table 2
Percentage in weight of $CO_3^=$

Size range	S1	S2	S3	S4
F4	86.20	92.80	76.80	63.50
F3	96.00	92.50	83.80	72.30
F2	92.80	96.60	84.10	74.10
F1	92.00	95.70	85.50	70.90
Mean [a]	91.80	94.40	82.50	70.20

[a] Over all families F_i.

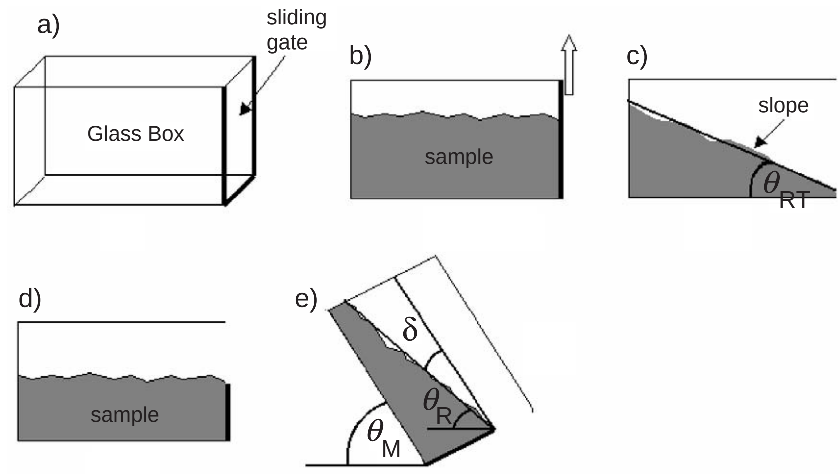

Fig. 2. Set-up used for measuring critical angles. (a) Glass box used for the determination of all angles; (b) front view of the box with the sample inside it; the right wall is being pulled upwards. (c) After the avalanche, the system relaxes to an angle θ_{RT}. (d) Front view of the box with the upper half of the right wall removed (bold line). This set-up is used to determine θ_R and θ_M. (e) After continuously tilting the wall, an avalanche occurs and rotation is stopped. Angles θ_R and θ_M are measured as indicated.

In some experiments local rearrangements of the free surface are observed before the avalanche, in agreement with the observations of Frette et al. [8]. These rearrangements can be easily distinguished from the avalanche itself which represents a “catastrophic” event.

Values obtained for samples S1 and S3 are displayed in Fig. 3a and b, respectively. These results correspond to experiments performed with the complete sample (all sizes included) and for subsets F4, F3 and F1–F2. These last two subsets were put together into the container in order to have enough material to determine precisely the slopes and to avoid fluctuations resulting from the large size of the grains. In this plot, we also show the difference $\delta = \theta_M - \theta_R$ between the angles θ_M and θ_R, i.e., $\delta = \theta_M - \theta_R$.

First of all, the behavior of both samples is practically the same and there is no substantial difference between the corresponding values. This means that the range of aspect ratios used here does not affect the stability of the heaps. In all cases, the values of the angles are large: θ_M, θ_R and θ_{RT} range between 40° and 60° due to the angular shape of the grains.

These angles also depend on grain size. Critical angles for the complete raw material are larger than those obtained for subsets F1–F2 and F3. Heaps made of grains belonging to these two subsets seem to be less stable. The stability seems therefore to be increased by the inclusion of fine material, i.e., dust from subset F4. The angle θ_{RT} measured for this subset is significantly larger than its value for other subsets and even for the complete sample. Including a large (almost 20%) amount of fine material should reduce both interactions between grains and differences due to their geometry. But no important differences associated to the shape were detected for subsets of grains of large sizes.

As observed in the figure, we only report values for the angle θ_{RT} for family F4. The other two angles, θ_R and θ_M, could not be measured with an adequate confidence (although, they always were pretty much higher than for other families) because the dynamics of this fine material was such that avalanches occurred as an entire block and the determination of the critical point at which they appeared was very difficult. Moreover, the

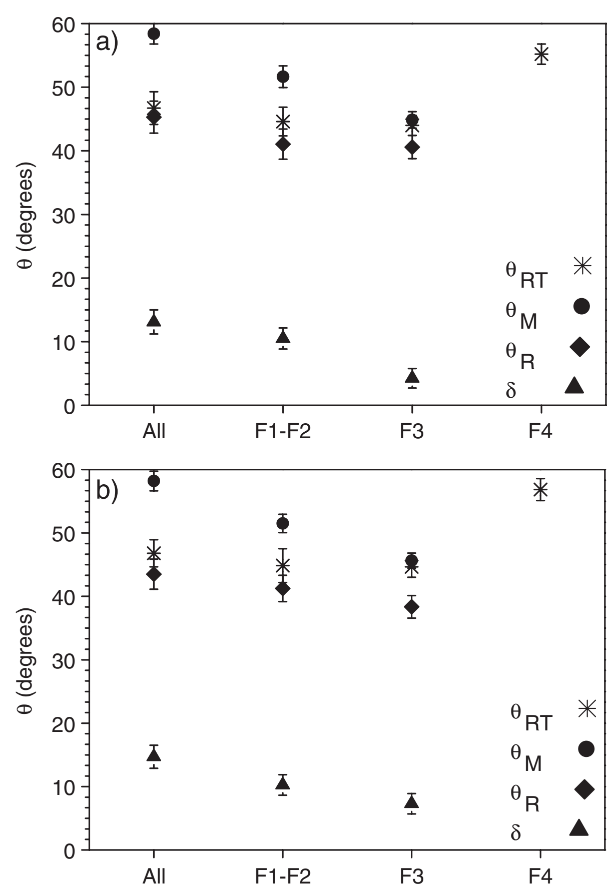

Fig. 3. Critical angles for sub-samples a) S1 and b) S3. “All” on the horizontal axis means “whole sample”, including all grain sizes. Bars indicate experimental error bounds.

Table 3
Percentage in weight for each of the different selected mixtures ratios

Mixture ratio	F1–F2	F3	F4
1	50	50	0
2	45	50	5
3	40	50	10
4	35	50	15
5	30	50	20
6	20	50	30
7	10	50	40

final free surface shape after the avalanche is in general irregular and convex.

At this stage, one wonders which results can be obtained by controlling the relative amounts of large grains, medium grains and dust in the mixture. A first indication on these issues has been obtained by analyzing the values of the characteristic angles of the heaps for different compositions. In view of the interplay between coarse grains and dust, we investigated more systematically the influence of the relative fractions corresponding to subsets F4 and F1–F2 one the values of the angles. To this end, we performed experiments, similar to the above ones, with mixtures including different relative amounts of these two families, keeping constant the relative amount of F3 grains. The percentages selected for the different mixtures are shown in Table 3. Due to the similar behavior of the different samples (Fig. 3), experiments were only performed for sample S1. We kept the total weight of each mixture constant and equal to 40 kg. For instance, mixture #1 was prepared with 50% of F1–F2 (20 kg) and 50% of F3 (20 kg); sample #2 with 45% of F1–F2 (18 kg), 50% of F3 (20 kg) and 5% of F4 (2 kg), and so forth. Mixtures including no large grains and only subsets F3 and F4, were avoided because of handling problems due to the large fraction of dust. In fact, measuring angles when fine grains are the main components of the mixture is, as said above, much complicated because of the blockage they induce.

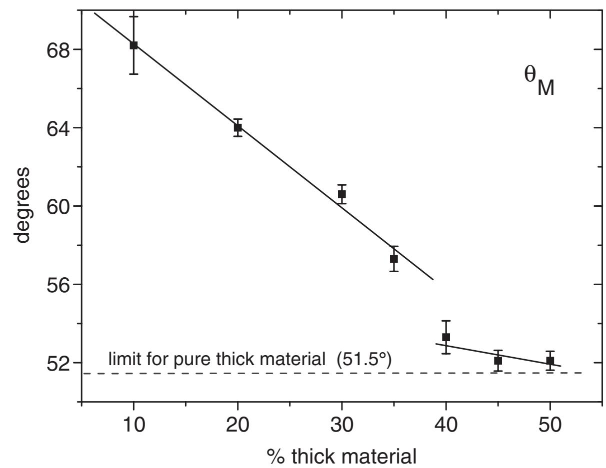

Fig. 5. Maximum angle of stability θ_M as a function of the fraction of coarse material (F1–F2). Lines indicate a least square fit. Bars indicate experimental error bounds.

The characteristic angles were measured for all mixture compositions and the results for θ_{RT}, θ_M and θ_R are displayed in Figs. 4–6, respectively.

As can be observed from the figures, it is angle θ_M that gets most affected by the addition of coarse grains and the removal of dust. Its value varies indeed by 16° when the percentage of fine material increases from 10% to 50%.

Angle θ_R has the most stable value and appears to be the most representative of a particular granular system. It remains practically constant until the amount of coarse material becomes larger than 30%. Above this percentage, its value only decreases by 8° until the value for pure material value is reached. On the other hand, θ_{RT} is not as stable as θ_R and displays a behavior similar to that of θ_M.

In all three figures, two variation regimes are observed for the angles: for a 30% fraction of coarse grains in the mixture there is a crossover between two regimes of variation of the angles. For θ_R, this change is important while, for the other two

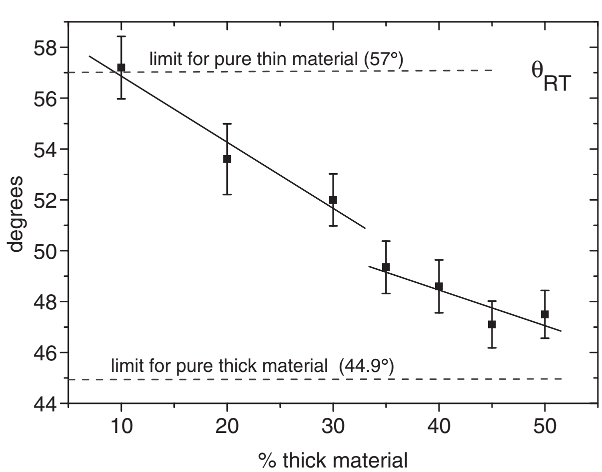

Fig. 4. Angle of repose θ_{RT} as a function of the fraction of fine material (F4) ratio. Lines indicate a least square fitting. Bars indicate experimental error bounds.

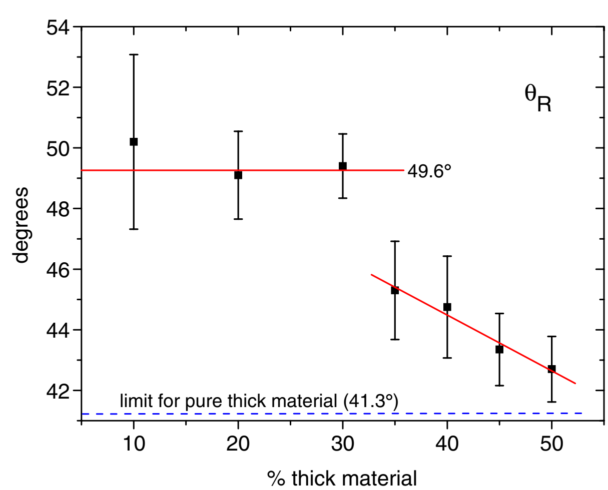

Fig. 6. Angle of repose θ_R as a function of the fraction of coarse material (F1–F2) ratio. Lines indicate a least square fit. Bars indicate experimental error bounds.

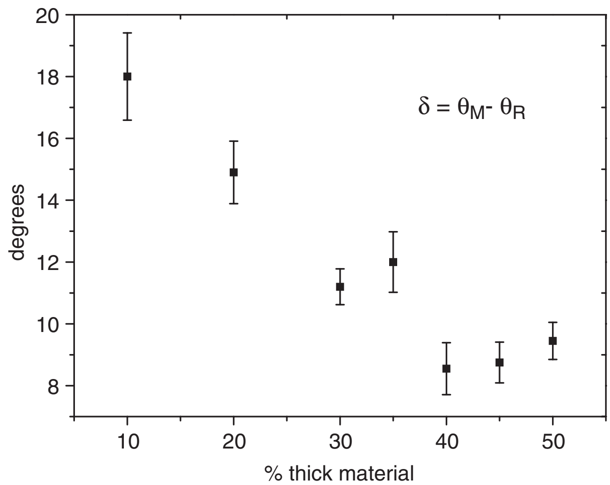

Fig. 7. Values for the difference $\delta = \theta_M - \theta_R$ as a function of coarse material (F1–F2) ratio. Bars indicate experimental error bounds.

angles, the slope is a slightly lower. Moreover, the variation of the three angles displays a sharp drop around a fraction 30%.

Increasing above 50% the fraction of weight corresponding to the coarse material practically does not influence the values of the angles. This is clearly appreciated in the figures by looking at the limiting values of the variation and comparing it to angles corresponding to pure fine and coarse material are indicated by dashed lines. This also means that the presence of intermediate sizes in those limiting cases does not affect the final values of the angles for pure fine or pure coarse materials.

Finally, the variation of $\delta = \theta_R - \theta_M$ is displayed in Fig. 7: they are of somewhat higher amplitude than those obtained for classical sand systems or glass beads.

3. Conclusions

Experiments have been performed with the actual granular materials used in cement manufacturing. This study has allowed one to correlate the critical angles of the packings to the shape and the chemical composition of the grains. It also allowed one to understand the influence of the mixture composition on the angles of stability of the heaps. The geometry of the grains has been found to be related to their chemical composition and, more specifically to the content of schist and limestone in the rock.

On the one hand, critical angles are nearly independent on the flatness and the elongation of the grains, at least for the range of parameters used here. On the other hand, they appear to be very sensitive to the distribution of their size.

θ_M is that of the angles which most affected by the addition of coarse grains and the removal of dust. Angle θ_R is found to be more stable and intrinsic to a particular granular system in agreement with the results other authors. θ_{RT} is not as stable as θ_R and displays a behavior similar to that of θ_M.

In most experiments reported here, the displacement of material during an avalanche is pretty much block-like and does not involve continuous surface motions (but for local rearrangements at the free surface). This might due to the broad dispersion of particle sizes and to its influence on the formation of the heap.

The fine grains added to bigger ones fills up the space between them (due to percolation effects, [14]) and change the properties of the initial packing (global and local compaction) resulting in an increase of the critical angles. This explains the large difference between θ_R and θ_M (8° to 18° in Fig. 7) which distinguishes this materials from other ones for which the difference δ of these angles of the order of 2° (rounded grains or sand [11,15]).

A final observation is the fact that large relative amount of dust, compared to that of coarse grains, stabilizes the granular packing.

As a future goal, we plan to measure the dependence of the degree of homogenization of a heap on its history formation and on the dispersion of grain sizes. This study will intend to bring light to some of the common chemical homogenization problems that the cement manufacturing industry has.

References

[1] H.M. Jaeger, S.R. Nagel, R.P. Behringer, Rev. Mod. Phys. 68 (1996) 1259.
[2] J. Duran, Sables, Poudres et Grains, Eyrolles, Paris, 1997.
[3] F.C. Franklin, L.N. Johanson, Chem. Eng. Sci. 4 (3) (1955) 119.
[4] S.R. Nagel, Rev. Mod. Phys. 64 (1992) 321.
[5] J. Lee, H.J. Herrmann, J. Phys., A 26 (1993) 373.
[6] F. Cantelaube, D. Bideau, Europhys. Lett. 30 (1995) 133.
[7] M.A. Aguirre, N. Nerone, A. Calvo, I. Ippolito, D. Bideau, Phys. Rev., E 62 (1) (2000) 738.
[8] V. Frette, K. Christensen, A. Malthesorenssen, J. Feder, T. Jossang, P. Meakin, Nature 379 (1996) 49.
[9] N. Nerone, M.A. Aguirre, A. Calvo, D. Bideau, I. Ippolito, Phys. Rev., E 67 (2003) 011302.
[10] P. Evesque, Phys. Rev., A 43 (1991) 2720.
[11] M.A. Aguirre, N. Nerone, I. Ippolito, A. Calvo, D. Bideau, Granul. Matter 3 (2001) 75.
[12] J.A. Drahun, J. Bridgwater, Powder Technol. 36 (1983) 39.
[13] J. Bridgwater, Powder Technol. 15 (1976) 215.
[14] J. Bridgwater, D. Ingram, Trans. Inst. Chem. Eng. 49 (1971) 163.
[15] S.R. Nagel, Rev. Mod. Phys. 64 (1992) 321.